

DOI: 10.13208/j.electrochem.141041

Artical ID:1006-3471(2015)02-0130-08

Cite this: *J. Electrochem.* **2015**, 21(2): 130-137

Http://electrochem.xmu.edu.cn

# 燃料电池非铂基氧还原电催化剂的最新研究进展

宋 平<sup>1,2</sup>, 阮明波<sup>1,2</sup>, 刘 京<sup>1,2</sup>, 冉光钧<sup>1,2</sup>, 徐维林<sup>1,2\*</sup>

(1. 中国科学院长春应用化学研究所, 电分析国家重点实验室, 吉林 长春 130022;

2. 中国科学院长春应用化学研究所, 吉林省低碳化学能源重点实验室, 吉林 长春 130022)

**摘要:** 目前, 燃料电池中广泛使用的Pt基阴极催化剂价格昂贵、资源缺乏, 且易中毒, 故急需开发廉价、耐用、高效和高耐醇的非铂基阴极氧还原催化剂. 本文阐述了国内外在非铂氧还原催化剂方面的研究, 并着重介绍了作者课题组的最新研究进展. 主要集中在非贵金属(Fe)负载和杂原子(F)掺杂的非金属催化剂, 力求原料廉价并可提高催化剂的催化活性、稳定性、抗毒化能力, 实现较高的性价比. 同时通过理论计算解释了氮单掺杂和氮氟共掺杂高效性的根源, 为设计高效催化剂提供了有力的理论支持.

**关键词:** 氧还原反应; 非贵金属催化剂; 非金属催化剂; 高性价比; 高稳定性; 催化机理; 理论水平

**中图分类号:** O646

**文献标识码:** A

燃料电池在动力电源、移动电子产品的便携式电源和小型发电装置等方面显示出极广阔的应用前景. 现今, 燃料电池发展和商业化的主要技术阻碍与难题有催化剂电催化活性低、阴极氧还原反应速率缓慢以及交换电流密度低等<sup>[1]</sup>, 制约了燃料电池电催化反应. 目前, 最好的直接甲醇燃料电池(DMFCs)阴极氧还原催化剂仍主要采用Pt/C催化剂. 然而Pt价格昂贵、成本过高, 且甲醇由于浓差扩散和电迁移透过质子交换膜渗透至阴极, 在阴极Pt催化剂上发生电氧化产生“混合电位”, 降低了电池开路电压和电池效率. 再者, 甲醇氧化的中间体CO很容易使Pt催化剂中毒. 因此, 开发廉价、耐用、高效和耐醇的非铂基阴极氧还原催化剂已经成为现今燃料电池研发的关键. 氧还原反应影响着燃料电池特性, 但其完整的氧还原反应机理及不同催化活性位点对氧气的作用过程等仍不明确, 因此, 从理论角度深入探讨反应机理、确定催化活性位点, 能更精准的解释实验事实, 并为实验设计优质催化剂提供有力的理论支持.

近来, 非铂基氧还原催化剂的研究主要集中在非贵金属(Fe、Co等)负载和杂原子(N、B、P、S、F

等)掺杂的非金属催化剂. 从上述两方面出发, 本文主要简述作者课题组近年取得的初步研究成果, 旨在降低阴极催化剂的成本, 提高催化剂活性和稳定性, 并展望今后非铂基氧还原催化剂的研究方向.

## 1 金属负载的氮掺杂催化剂

金属负载的氮掺杂催化剂的研究始于金属N<sub>4</sub>大环类化合物. 1964年, 美国科学家Jasinsky<sup>[2]</sup>首次合成一类酞菁钴(CoPc)化合物, 对氧还原反应具有较高的催化活性. 自此, 过渡金属大环化合物的非金属催化剂引起研究者广泛关注. 酞菁、卟啉及其衍生物等大环化合物已大量应用于Fe、Co等过渡金属N<sub>4</sub>大环化合物的研制, 并已证实M-N<sub>4</sub>活化位点有很高的反应活性<sup>[3-4]</sup>. Dodelet课题组<sup>[5]</sup>将石墨化碳材料、铁前驱体与孔填充剂一起球磨热解, 石墨化碳材料间的裂缝孔隙可被孔填充剂填充, 热解促进石墨层生长、孔隙微孔化, 实现铁与边缘吡啶氮的配位. 此类Fe/N/C催化剂的氧还原催化活性很高, H<sub>2</sub>-O<sub>2</sub>燃料电池最大功率密度高达750 mA·cm<sup>-2</sup>. Zelenay课题组<sup>[6]</sup>将苯胺齐聚物实现聚苯胺化并包裹于高表面积碳纳米材料和过渡金属前驱体

收稿日期: 2014-10-10, 修订日期: 2014-11-20 \* 通讯作者, Tel: (86-431)85262848, E-mail: weilinxu@ciac.ac.cn

国家重点基础研究发展计划(No. 2012CB932800, No. 2014CB932700), 国家自然科学基金项目(No. 21273220, No. 21073180)和“青年千人计划”资助

上,热解产物在 $0.5 \text{ mol} \cdot \text{L}^{-1} \text{H}_2\text{SO}_4$ 中除去不稳定和非氧还原活性的相,而后再次热解.此非贵金属催化剂有很高的燃料电池功率和稳定性,其副产物双氧水的产率低于1%. Müllen和冯新亮课题组<sup>[7]</sup>合作,用维生素B12与聚苯胺铁在一系列模板剂条件下制得过渡金属负载的介孔催化剂,在酸性条件下有很高的催化活性、选择性和稳定性,这主要取决于较高表面积的介孔分布结构及大量的M-N<sub>x</sub>活性位点.接着,他们又在无模板条件下用钴卟啉和有机配合物形成的共轭介孔聚合物,经高温热解得到带状的钴氮共掺杂的碳催化剂<sup>[8]</sup>.该催化剂具有大比表面积的微孔结构,在碱性条件下显示出高催化活性.

金属卟啉的大环结构合成繁琐,且M-N<sub>x</sub>的活性结构易水解.为此,通过将M-N<sub>4</sub>结构嵌入到多孔碳材料中并高温热解可得M-N-C杂化材料,提高催化剂的活性和稳定性.作者课题组<sup>[9]</sup>利用炭黑、三聚氰胺以及三氯化铁等廉价的原料和简单球磨制

得一类痕量铁的Fe-N-C杂化介孔材料,系统研究了热解温度、氮源和碳源的质量比及铁最终含量等对氧还原催化活性的影响,发现900 °C热解、原料的碳氮比为1:10、最终铁含量为0.05%的催化剂活性最高(图1A).通过旋转圆盘电极(RDE)测试得到这种Fe-N-C催化剂的起始电位(vs. SCE)高达45 mV,其性能远超过商业碳载铂(图1B).据Koutecky-Levich (K-L)方程分析,该催化剂的表观电子转移数接近4e,基本是4电子氧还原过程,主要产物是水.此类催化剂对CO几乎无任何响应,而CN<sup>-</sup>的加入使催化活性大幅度降低(图1B、C),证实了体系的催化活性主要源于Fe-N<sub>x</sub>活性位点. Fe-N-C催化剂直接甲醇燃料电池的最大功率密度在相同测试条件下类似商业碳载铂(图1D),因此它是有利的替代商业碳载铂的非贵金属氧还原催化剂.此外,作者课题组计划通过预处理碳支撑材料、改变反应条件和氮前驱体等方法,以期得到稳定性更好、活性更高的铁载氮掺杂的非贵金属氧还原催化剂.

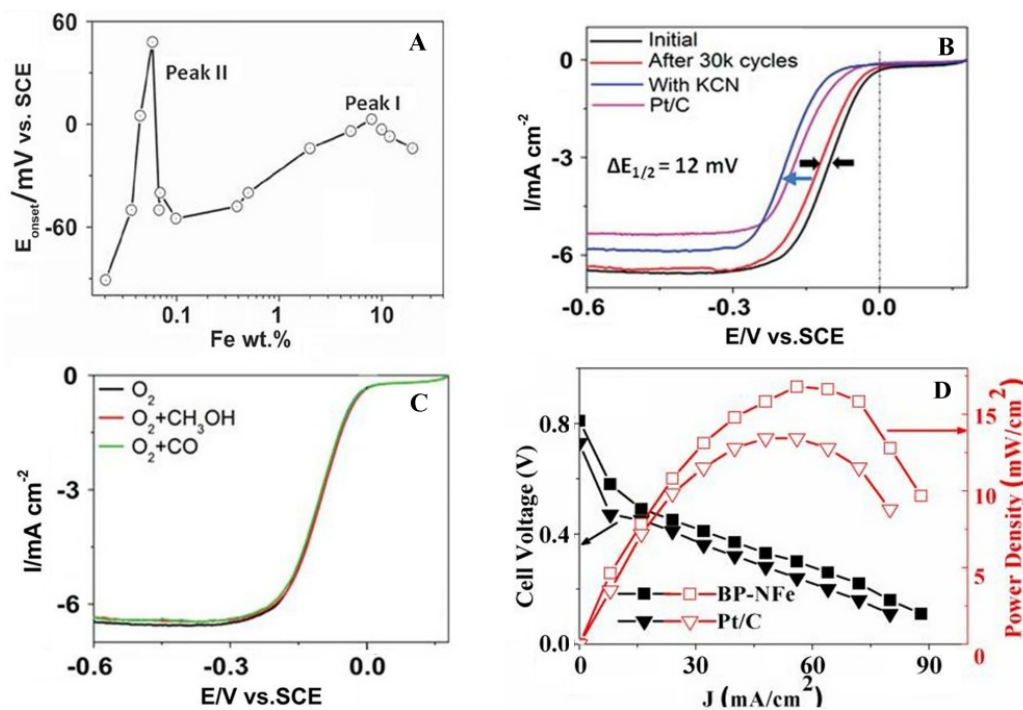


图1 A. 不同铁含量催化剂的起始电位值;B. BP-NFe催化剂在扫描30000圈前后以及加入CN<sup>-</sup>后的RDE极化曲线,并与商业Pt/C对比;C. BP-NFe催化剂的抗甲醇毒化曲线;D. 60 °C下CBP-NFe和Pt/C的ADMFCs电池电压和功率密度曲线<sup>[9]</sup>

Fig. 1 A. Fe-content dependent on set potentials of BP-NFe catalysts; B. RDE polarization curves of BP-NFe with a scan rate of  $5 \text{ mV} \cdot \text{s}^{-1}$  before and after 30000 potential cycles in  $\text{O}_2$ -saturated  $0.1 \text{ mol} \cdot \text{L}^{-1} \text{KOH}$ , and then KCN was added; C. The tolerance and stability of BP-NFe in  $\text{O}_2$ -saturated,  $3 \text{ mol} \cdot \text{L}^{-1}$  methanol  $\text{O}_2$ -saturated and  $\text{CO-O}_2$  saturated  $0.1 \text{ mol} \cdot \text{L}^{-1} \text{KOH}$ ; D. The cell voltage and power density curves of ADMFCs at  $60^\circ \text{C}$  with optimal BP-NFe ( $3 \text{ mg} \cdot \text{cm}^{-2}$ ) (square) and Pt/C (60%, by mass,  $3 \text{ mgPt} \cdot \text{cm}^{-2}$ ) (star) as cathodes, respectively<sup>[9]</sup>

## 2 非金属氧还原催化剂

目前非贵金属氧还原催化剂已受广泛关注,但在酸性介质中其循环稳定性差,成本较高,危害环境,影响了燃料电池的大量商业化.因此,开发非金属的氧还原催化剂燃料电池尤为重要.非金属催化剂研究主要集中于N、B、P、S和F等杂原子掺杂的碳材料.其中,六角形格子的单层碳原子排列的石墨烯具有高热稳定性以及独特的力学性质和电子性质,成为杂原子掺杂材料的首选.近年来,各种碳纳米结构如氧化或还原的石墨烯、石墨烯量子点、多层石墨、碳纳米管、碳纳米笼、碳纳米带、纳米多孔碳及碳化氮材料等,逐渐被用于杂原子掺杂的氧还原催化剂的制备<sup>[10-14]</sup>.

### 2.1 氮掺杂的氧还原催化剂

2006年,Ozkan等<sup>[15]</sup>首次制得完全氮掺杂的非金属氧还原催化剂,证实了氮掺杂在催化活性中的有效性,同时揭示了碳层边缘的吡啶氮在氧还原催化活性中的关键性作用:氮原子高的电负性使周边碳原子的电荷发生变化,从而增强了氧气在催化剂表面的吸附.自此,杂原子掺杂的氧还原催化剂获得广泛的关注.Dai课题组<sup>[16]</sup>通过热解一种铁酞菁类的金属杂环化合物,经电化学纯化除掉铁元素,得到垂直排列的氮掺杂的碳纳米管(VA-NCNTs)(图2A).首次在碱性条件下实现非金属催化剂的催化活性超过商业铂碳,这是氮掺杂非金属催化剂的一大突破(图2B).此类氮掺杂碳纳米管有很好的长期稳定性和强的抗交叉能力.据理论计算,其电负性强的氮原子使周边的碳原子的正电荷密度增加,且其特殊的垂直排列结构使该催化剂趋于4电子

过程.目前,已有研究者开始构筑二维或三维石墨烯纳米多孔结构以实现氮掺杂的氧还原催化剂.此类多维结构比表面积大、电导率高、电化学稳定性优良、催化活性较高<sup>[17]</sup>.此外,氮掺杂的三维聚合物、碳纳米胶囊及碳纳米管杯已先后被开发,并证实其对氧还原反应具有较高的活性<sup>[18-21]</sup>.氮掺杂的氧还原催化剂中氮的种类一般有吡啶氮、吡咯氮、石墨化氮以及氧化的氮等,但其中起活性作用的氮形式仍存在争议,因此关于氮掺杂催化体系的催化机理的理论计算应运而生.Lee和Zheng课题组<sup>[22-23]</sup>分别研究了氮掺杂碳纳米管的氧还原催化活性位点及催化机理.此外,吡啶氮<sup>[24-25]</sup>、石墨化的氮<sup>[26]</sup>也被视为催化活性的活性位点.因此,氧还原的氮掺杂体系的催化机理仍有待于完善.然不论如何,氮掺杂的氧还原催化剂是很有前途的燃料电池氧还原非金属催化剂.

### 2.2 硼、磷、硫单掺杂及其与氮共掺杂的氧还原催化剂

硼元素的缺电子特点可用以改性纯的碳材料,并应用于非金属氧还原催化剂.Hu课题组<sup>[27]</sup>用化学气相沉积法制得硼掺杂的碳纳米管,硼含量增加,其氧还原催化活性也随之提高,揭示了硼元素存在的重要性.据理论计算证实,电负性小于碳的硼元素所带的正电荷更有利于氧气在其表面的吸附,硼活性位点可在还原过程作为电子供体从而提升催化活性.其后,硼掺杂的金刚石、碳纳米管、石墨烯片等有效的非金属氧还原催化剂已被陆续开发<sup>[28-31]</sup>.

理论计算已证实磷元素的参与可有效地提升

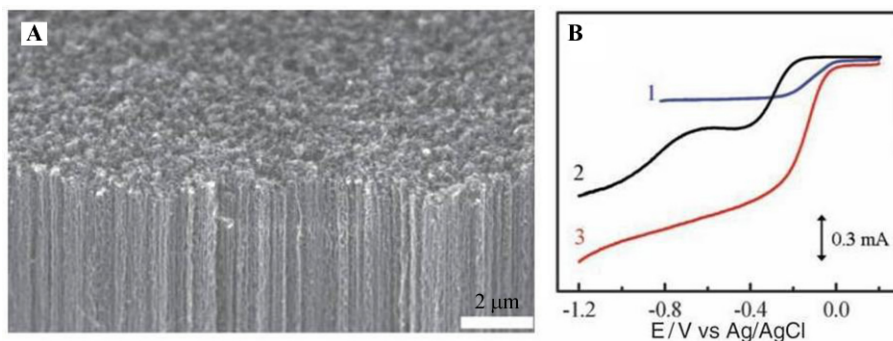


图2 A. 石英管底部合成的垂直排列的氮掺杂碳纳米管扫描电镜照片; B. Pt-C/GC(1)、VA-CCNT/GC(2)和VA-NCNT(3)电极在空气饱和的 $0.1 \text{ mol} \cdot \text{L}^{-1}$  KOH溶液的旋转环盘(RRDE)极化曲线<sup>[16]</sup>

Fig. 2 A. SEM image of the as-synthesized VA-NCNTs on a quartz substrate; B. RRDE voltammograms for oxygen reduction in air-saturated  $0.1 \text{ mol} \cdot \text{L}^{-1}$  KOH at the Pt-C/GC (curve 1), VA-CCNT/GC (curve 2), and VA-NCNT (curve 3) electrodes<sup>[16]</sup>



碳材料的供电子能力,从而提高催化活性.2011年,Peng等<sup>[32]</sup>制得磷掺杂的石墨片状材料,在碱性电介质中有较高的电催化活性、稳定性及抗甲醇特性.在原体系加入二茂铁得到磷掺杂的多壁碳纳米管,热解温度可调控纳米管的直径尺寸大小.此类含少量磷的碳纳米管的催化活性在碱性条件下超过了商业碳载铂,而其中残留金属的作用仍有待探讨.最近,Yu课题组<sup>[33]</sup>利用SBA-15模板制得磷掺杂的介孔碳材料,确保该催化剂只有磷的作用从而避免了金属对氧还原活性的影响.通过X-射线光电子能谱(XPS)证实,在磷掺杂的催化剂中磷主要以P—O和P—C形式存在.磷的掺杂比纯的碳材料的催化活性有明显提高,且比商业碳载铂更稳定、抗毒性更强.

与氮、硼和磷掺杂等相比,硫掺杂的碳材料目前仍比较稀缺,尤其是应用于氧还原催化剂.Denis等<sup>[34]</sup>通过理论计算发现因硫的尺寸及不同的结合方式使其掺杂较氮等更困难.Huang等<sup>[35]</sup>通过热解均相的氧化石墨烯和苯甲基二硫化物的混合物制得硫掺杂的石墨烯氧还原催化剂,在碱性条件下催化剂显示出较好的氧还原催化活性,属一类4电子还原的催化剂.近期,Chen等<sup>[36]</sup>用一步溶剂热原位掺杂硫合成了硫掺杂的石墨烯泡沫.Zhang等<sup>[37]</sup>以723-型的硫酸基酸性离子交换树脂制得的三维硫掺杂石墨烯有很高的比表面积和结晶度,在碱性条件下该催化活性可以与商业碳载铂相媲美,且具有更高的稳定性和抗甲醇毒性.Xia课题组<sup>[38]</sup>理论计算结合实验解释了硫掺杂的催化机理,硫掺杂增强硫周边碳原子的电荷和自旋密度,有利于氧气的吸附和4电子还原过程.

B、P、S元素与N元素的电负性有差异,利用这几种元素与氮元素的协同效应和独特的电子结构,可以改善目前的碳材料,实现多元掺杂.目前,大多数杂原子掺杂的碳材料尤其纳米管和石墨烯均经真空下化学气相沉积法制得,该法繁琐昂贵<sup>[39]</sup>.2012年,Dai课题组<sup>[40]</sup>制得可调控的硼氮共掺杂的石墨烯催化剂,其催化活性和稳定性超过目前的商业碳载铂.同时,理论计算还揭示硼氮共掺杂的协同效应可调控能带、自旋密度以及电荷密度,通过调节掺杂的硼氮比例可得到最好性能的催化剂.最近,Sun等<sup>[41]</sup>用廉价的尿素、硼酸及聚乙烯为前驱体制得褶皱的硼氮共掺杂的石墨层状结构,显示了高稳定活性、抗甲醇毒性及四电子反应特性,

证实两种及其以上的元素的协同效应可更好提高氧还原催化剂的催化活性.自此,磷氮以及硫氮等共掺杂的非金属催化剂已被大量尝试.Zhu等<sup>[42]</sup>通过简单的一锅法制得有很大内通道的氮磷共掺杂的碳纳米管,允许氧分子接触至内壁的大量活性位点,从而提升催化活性.氮磷的协同效应使该催化剂稳定性超高,抗甲醇毒性亦很强.硫氮的共掺杂催化剂方面也已取得突出的成果.Qiao课题组<sup>[43]</sup>用一步法制得介孔硫氮共掺杂的石墨烯碳材料,显示出较好的催化活性.Huang课题组<sup>[44]</sup>将廉价的介孔硅、蔗糖和和硫脲的混合物经简单高温热解、HF刻蚀硅,得到三维多孔的硫氮共掺杂的碳泡沫.这些分级别的三维孔状结构可确保氧还原过程的电子转移和反应物传输速率,改善催化剂的稳定性.硫氮的协同效应则使该催化剂有很高的催化活性.

## 2.3 氟原子掺杂及氮氟共掺杂的氧还原催化剂

氟元素作为电负性很强的原子,近年已用于非金属氧还原催化剂的研究.此前,Jeon等<sup>[45]</sup>通过球磨 $\text{Cl}_2$ 、 $\text{Br}_2$ 、 $\text{I}_2$ 和石墨,得到边缘卤化的石墨烯.然而氟气分子活泼,毒性大,此法不可能得到氟化的石墨烯.2013年,Xu课题组<sup>[46]</sup>研发了一种简单易行的掺杂氟的方法.用廉价的炭黑做碳源、氟化铵做氟源,通过高温 $1000\text{ }^\circ\text{C}$ 的热解得到了首例氟掺杂的氧还原碳材料催化剂.通过简单的碳氟比例调控,得到一系列活性不同的氟掺杂碳材料.氟的引入增加了碳材料本身的石墨化程度,产生更多的介孔和缺陷结构,更有利于改善催化性能.此类氟掺杂的催化剂活性在碱性条件下超过了商业碳载铂,且有很好的稳定性和抗毒性(图3A).据K-L方程得到此类氟掺杂的催化剂的氧还原催化过程几乎是一个四电子过程,其高活性和高选择性主要源于半离子态的C—F键的形成以及氟掺杂造成的更多的缺陷位点(图3B、C).此类掺杂氟的催化剂在酸性条件下也显示较高的活性和抗毒性,双氧水产量超低( $<0.1\%$ )(图3D)<sup>[47]</sup>.理论计算发现,氟的引入降低了体系的能隙,且氟的强电负性使周围的碳原子正电荷增加,增强了氧气在其表面的吸附,削弱了O—O键,更利于氧气还原.

当氮氟共掺杂时,氧气的吸附能进一步增加,O—O键进一步削弱,预示着氮氟共掺杂体系应该比氟掺杂或氮掺杂具有更高的催化活性.据此理

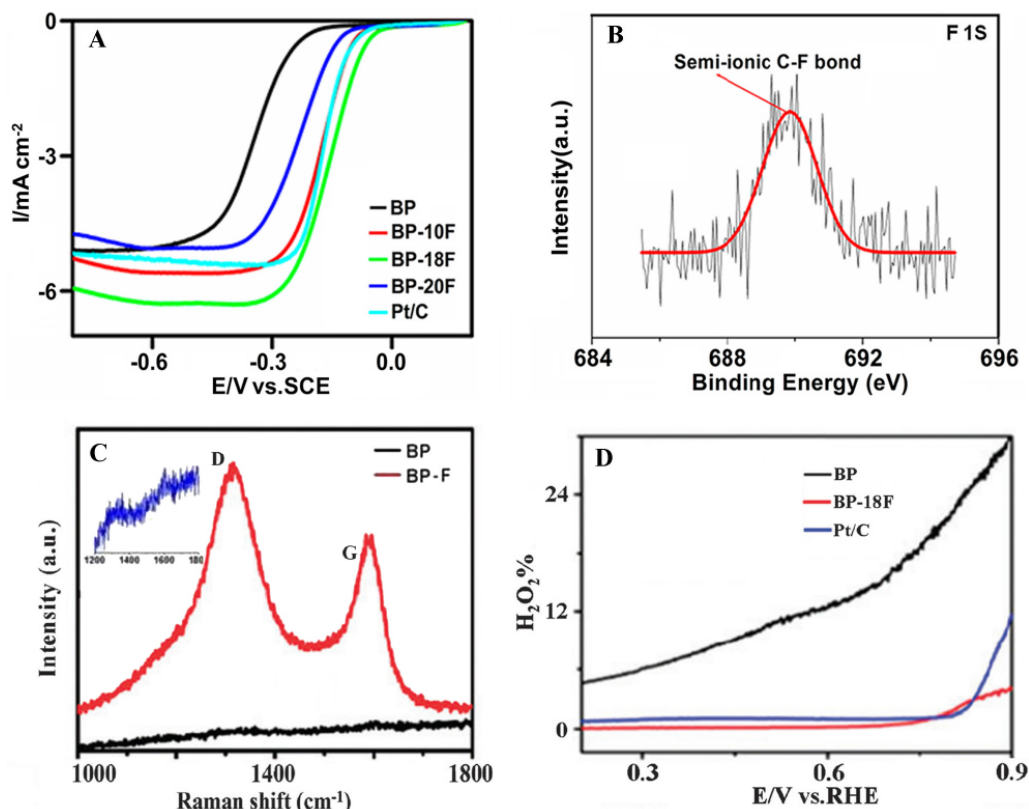


图3 A. 不同F含量的BP-F催化剂及20%(by mass)铂在氧气饱和的 $0.1 \text{ mol} \cdot \text{L}^{-1}$  KOH溶液中的RRDE极化曲线,旋转速率为 $1600 \text{ r} \cdot \text{min}^{-1}$ ,扫描速率为 $5 \text{ mV} \cdot \text{s}^{-1}$ [46]; B. F 1s的高分辨XPS光谱(插图为黑线BP的放大图)[46]; C. BP和BP-18F催化剂的Raman光谱[46]; D. BP、BP-18F和Pt/C在 $0.5 \text{ mol} \cdot \text{L}^{-1}$   $\text{H}_2\text{SO}_4$ 溶液中的双氧水含量[47]

Fig. 3 A. Linear sweep curves of different BP-F catalysts and 20% (by mass) Pt in  $\text{O}_2$ -saturated  $0.1 \text{ mol} \cdot \text{L}^{-1}$  KOH with a rotation rate of  $1600 \text{ r} \cdot \text{min}^{-1}$  and a scan rate of  $5 \text{ mV} \cdot \text{s}^{-1}$  [46]; B. high-resolution XPS spectrum of F 1s [46]; C. Raman spectra for BP and BP-18F catalysts (the inset is the magnification of the black line for BP) [46]; D.  $\text{H}_2\text{O}_2$  yields of the catalysts calculated from RRDE curves in  $0.5 \text{ mol} \cdot \text{L}^{-1}$   $\text{H}_2\text{SO}_4$  at  $1600 \text{ r} \cdot \text{min}^{-1}$  [47]

论预测,可调控上述反应,首先将炭黑和氮源三聚氰胺高温热解,再将所得氮掺杂样品加入氟化铵分步热解[48]。据XPS分析,该体系同时含有C、O、N和F,即首次实现了氮氟共掺杂。氮氟共掺杂效应使碳材料的结构由微孔变为更有利于其反应活性的介孔,氧还原催化活性确实高于氟掺杂和氮掺杂,也高于商业碳载铂,与理论计算一致(图4A)。此类氮氟共掺杂的体系50000周期循环后其活性基本不下降,对甲醇抗毒化性很强(图4B),直接甲醇燃料电池的开路电压和最大功率密度均超过了目前的商业碳载铂(图4C、D),有望成为最有潜力的替代铂基的氧还原催化剂。

### 3 总结与展望

开放低成本高效能的非铂基阴极氧还原催化剂是解决铂资源短缺、促进燃料电池产业化的重

要途径。非铂基氧还原催化剂主要有非贵金属负载和非金属掺杂两大类:

1)非贵金属氧还原催化剂主要通过高温热解过渡金属前驱体、氮源和碳源的混合物制得。杂原子掺杂的非金属催化剂则需要选取合适的廉价杂原子前驱体,经较简单方法(热解或溶剂热等)制得单掺杂或多元掺杂的催化剂,尽可能实现较高的性价比和环境友好等特点。

2)催化剂的设计应力求使氧分子在催化剂表面趋向4电子反应,以提高反应效率。理论计算尤为重要,目前氧还原催化剂的催化机理和催化活性尚未明确阐述。理论与实验相结合,通过模拟可能的催化活性位点,初判反应机理,阐述催化剂结构和催化性能的相互关系,以期指导实验、优化制备条件。

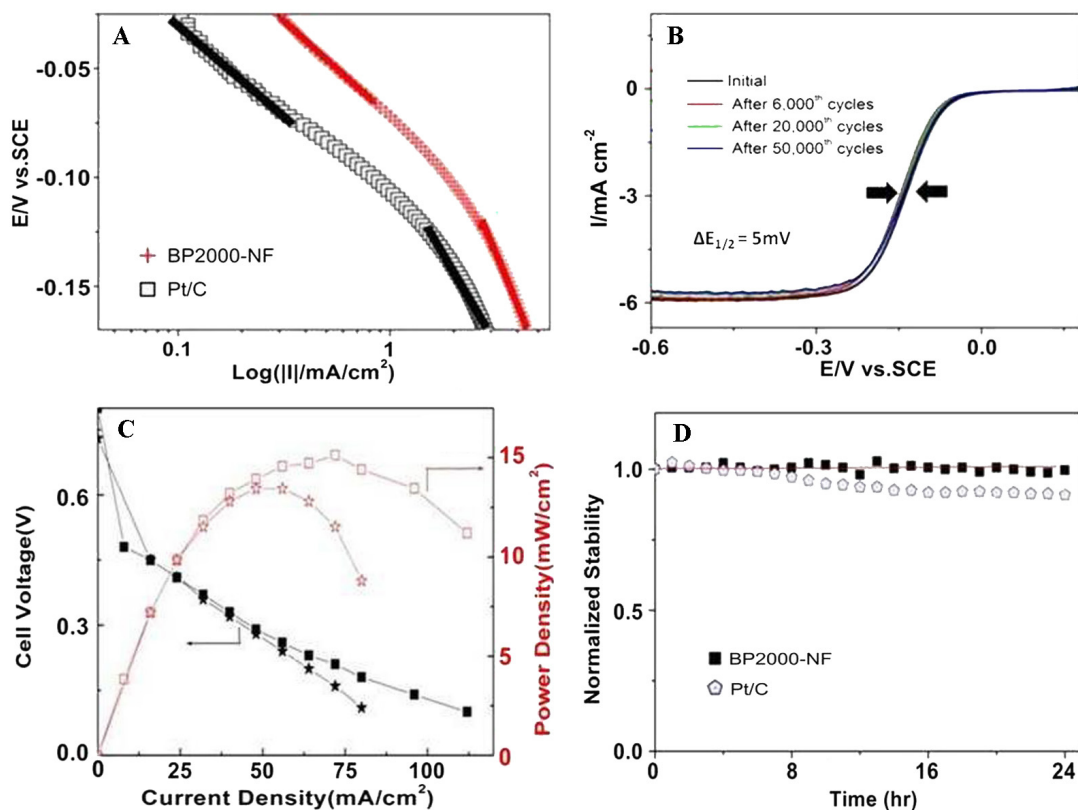


图4 A. BP2000-NF和Pt/C催化剂的Tafel曲线;B. 0.1 mol·L⁻¹ KOH溶液中BP2000-NF催化剂在分别扫描6000、20000和50000圈前后的RDE极化曲线(扫描速率为5 mV·s⁻¹);C. BP2000-NF(方形)和Pt/C(星状)的ADMFCs在60 °C下的开路电压和功率密度曲线;D. BP2000-NF和Pt/C催化剂的归一化寿命曲线(37 °C, 200 mA)<sup>[48]</sup>

Fig. 4 A. Tafel plots for BP2000-NF and Pt/C; B. RDE polarization curves of BP2000-NF with scan rate of 5 mV·s⁻¹ before and after 6 000, 20 000 and 50 000 potential cycles in O₂-saturated 0.1 mol·L⁻¹ KOH; C. The cell voltage and power density curves of ADMFCs at 60 °C with BP2000-NF (3 mg·cm⁻²) (square) and Pt/C (60% by mass, 3 mgPt·cm⁻²) (star) as cathodes, respectively; D. The normalized long-term operation stability of ADMFC potential using BP2000-NF and Pt/C as cathodes, respectively, with fixed current of 200 mA at 37 °C. Anode: Pt/C (60 % by mass, 3 mgPt·cm⁻²) with 2 mol·L⁻¹ methanol in 2 mol·L⁻¹ KOH and a flow rate of 5 mL·min⁻¹, cathode: dry oxygen with flow rate of 100 mL·min⁻¹<sup>[48]</sup>

为实现燃料电池催化剂的更佳设计和制备, 上述问题仍需有效地解决, 这将对燃料电池催化剂的商业化进程产生更快的推动作用。

### 参考文献(References):

- [1] Morozan A, Josselme B, Palacin S. Low-platinum and platinum-free catalysts for the oxygen reduction reaction at fuel cell cathodes[J]. *Energy & Environmental Science*, 2011, 4(4): 1238-1254.
- [2] Jasinski R. A new fuel cell cathode catalyst[J]. *Nature*, 1964, 201(4925): 1212-1213.
- [3] Tian J, Morozan A, Sougrati M T, et al. Optimized synthesis of Fe/N/C cathode catalysts for PEM fuel cells: A matter of iron-ligand coordination strength[J]. *Angewandte Chemie International Edition*, 2013, 52(27): 6867-6870.
- [4] Hu Y, Jensen J O, Zhang W, et al. Hollow spheres of iron carbide nanoparticles encased in graphite layers as oxygen reduction catalysts[J]. *Angewandte Chemie International Edition*, 2014, 53(14): 3675-3679.
- [5] Lefèvre M, Proietti E, Jaouen F, et al. Iron-based catalysts with improved oxygen reduction activity in polymer electrolyte fuel cells[J]. *Science*, 2009, 324(5923): 71-74.
- [6] Wu G, More K L, Johnston C M, et al. High-performance electrocatalysts for oxygen reduction derived from polyaniline, iron, and cobalt[J]. *Science*, 2011, 332(6028): 443-447.
- [7] Liang H W, Wei W, Wu Z S, et al. Mesoporous metal-nitrogen-doped carbon electrocatalysts for highly efficient oxygen reduction reaction[J]. *Journal of The American Chemical Society*, 2013, 135(43): 16002-16005.
- [8] Wu Z S, Chen L, Liu J, et al. High-performance electrocat-

- alysts for oxygen reduction derived from cobalt porphyrin-based conjugated mesoporous polymers[J]. *Advanced Materials*, 2014, 26(9): 1450-1455.
- [9] Liu J, Sun X, Song P, et al. High-performance oxygen reduction electrocatalysts based on cheap carbon black, nitrogen, and trace iron[J]. *Advanced Materials*, 2013, 25(47): 6879-6883.
- [10] Liu Z W, Peng F, Wang H J, et al. Phosphorus-doped graphite layers with high electrocatalytic activity for the O<sub>2</sub> reduction in an alkaline medium[J]. *Angewandte Chemie International Edition*, 2011, 50: 3257-3261.
- [11] Liu Z W, Peng F, Wang H J, et al. Novel phosphorus-doped multiwalled nanotubes with high electrocatalytic activity for O<sub>2</sub> reduction in alkaline medium[J]. *Catalysis Communications*, 2011, 16(1): 35-38.
- [12] Li Q, Zhang S, Dai L, et al. Nitrogen-doped colloidal graphene quantum dots and their size-dependent electrocatalytic activity for the oxygen reduction reaction[J]. *Journal of The American Chemical Society*, 2012, 134(46): 18932-18935.
- [13] Zhang C, Mahmood N, Yin H, et al. Synthesis of phosphorus-doped graphene and its multifunctional applications for oxygen reduction reaction and lithium ion batteries[J]. *Advanced Materials*, 2013, 25(35): 4932-4937.
- [14] Liu Z, Peng F, Wang H, et al. Preparation of phosphorus-doped carbon nanospheres and their electrocatalytic performance for O<sub>2</sub> reduction[J]. *Journal of Natural Gas Chemistry*, 2012, 21(3): 257-264.
- [15] Matter P H, Ozkan U S. Non-metal catalysts for dioxygen reduction in an acidic electrolyte[J]. *Catalysis letters*, 2006, 109(3/4): 115-123.
- [16] Gong K, Du F, Xia Z, et al. Nitrogen-doped carbon nanotube arrays with high electrocatalytic activity for oxygen reduction[J]. *Science*, 2009, 323(5915): 760-764.
- [17] Ito Y, Qiu H J, Fujita T, et al. Bicontinuous nanoporous N-doped graphene for the oxygen reduction reaction[J]. *Advanced Materials*, 2014, 26(24): 4145-4150.
- [18] Wang S, Yu D, Dai L. Polyelectrolyte functionalized carbon nanotubes as efficient metal-free electrocatalysts for oxygen reduction[J]. *Journal of The American Chemical Society*, 2011, 133(14): 5182-5185.
- [19] Shanmugam S, Osaka T. Efficient electrocatalytic oxygen reduction over metal free-nitrogen doped carbon nanocapsules [J]. *Chemical Communications*, 2011, 47(15): 4463-4465.
- [20] Tang Y, Allen B L, Kauffman D R, et al. Electrocatalytic activity of nitrogen-doped carbon nanotube cups[J]. *Journal of The American Chemical Society*, 2009, 131(37): 13200-13201.
- [21] He W, Jiang C, Wang J, et al. High-rate oxygen electroreduction over graphitic-N species exposed on 3D hierarchically porous nitrogen-doped carbons[J]. *Angewandte Chemie-International Edition*, 2014, 53(36): 9503-9507.
- [22] Lee W J, Maiti U N, Lee J M, et al. Nitrogen-doped carbon nanotubes and graphene composite structures for energy and catalytic applications[J]. *Chemical Communications*, 2014, 50(52): 6818-6830.
- [23] Zheng Y, Jiao Y, Jaroniec M, et al. Nanostructured metal-free electrochemical catalysts for highly efficient oxygen reduction[J]. *Small*, 2012, 8(23): 3550-3566.
- [24] Sheng Z H, Shao L, Chen J J, et al. Catalyst-free synthesis of nitrogen-doped graphene via thermal annealing graphite oxide with melamine and its excellent electrocatalysis[J]. *ACS Nano*, 2011, 5(6): 4350-4358.
- [25] Qu L, Liu Y, Baek J B, et al. Nitrogen-doped graphene as efficient metal-free electrocatalyst for oxygen reduction in fuel cells[J]. *ACS Nano*, 2010, 4(3): 1321-1326.
- [26] Liu R, Wu D, Feng X, et al. Nitrogen-doped ordered mesoporous graphitic arrays with high electrocatalytic activity for oxygen reduction[J]. *Angewandte Chemie International Edition*, 2010, 49(14): 2565-2569.
- [27] Yang L J, Jiang S J, Zhao Y, et al. Boron-doped carbon nanotubes as metal-free electrocatalysts for the oxygen reduction reaction[J]. *Angewandte Chemie International Edition*, 2011, 50(31): 7132-7135.
- [28] Yang L, Jiang S, Zhao Y, et al. Boron-doped carbon nanotubes as metal-free electrocatalysts for the oxygen reduction reaction[J]. *Angewandte Chemie International Edition*, 2011, 50(31): 7132-7135.
- [29] Sheng Z H, Gao H L, Bao W J, et al. Synthesis of boron doped graphene for oxygen reduction reaction in fuel cells[J]. *Journal of Materials Chemistry*, 2012, 22(2): 390-395.
- [30] Szunerits S, Manesse M, Actis P, et al. Influence of the surface termination of boron-doped diamond electrodes on oxygen reduction in basic medium[J]. *Electrochemical and Solid State Letters*, 2007, 10(7): G43-G46.
- [31] Ernst S, Aldous L, Compton R G. The electrochemical reduction of oxygen at boron-doped diamond and glassy carbon electrodes: A comparative study in a room-temperature ionic liquid[J]. *Journal of Electroanalytical Chemistry*, 2011, 663(2): 108-112.
- [32] Liu Z W, Peng F, Wang H J, et al. Phosphorus-doped graphite layers with high electrocatalytic activity for the O<sub>2</sub> reduction in an alkaline medium[J]. *Angewandte Chemie International Edition*, 2011, 50(14): 3257-3261.
- [33] Yang D S, Bhattacharjya D, Inamdar S, et al. Phosphorus-doped ordered mesoporous carbons with different lengths as efficient metal-free electrocatalysts for oxygen reduction reaction in alkaline media[J]. *Journal of The American Chemical Society*, 2012, 134(39): 16127-16130.
- [34] Denis P A, Faccio R, Mombru A W. Is it possible to dope



- single-walled carbon nanotubes and graphene with sulfur?[J]. *ChemPhysChem*, 2009, 10(4): 715-722.
- [35] Yang Z, Yao Z, Li G, et al. Sulfur-doped graphene as an efficient metal-free cathode catalyst for oxygen reduction [J]. *ACS Nano*, 2011, 6(1): 205-211.
- [36] Chen L, Cui X, Wang Y, et al. One-step synthesis of sulfur doped graphene foam for oxygen reduction reactions [J]. *Dalton Transactions*, 2014, 43(9): 3420-3423.
- [37] Zhang Y, Chu M, Yang L, et al. Synthesis and oxygen reduction properties of three-dimensional sulfur-doped graphene networks[J]. *Chemical Communications*, 2014, 50(48): 6382-6385.
- [38] Zhang L, Niu J, Li M, et al. Catalytic mechanisms of sulfur-doped graphene as efficient oxygen reduction reaction catalysts for fuel cells[J]. *The Journal of Physical Chemistry C*, 2014, 118(7): 3545-3553.
- [39] Hata K, Futaba D N, Mizuno K, et al. Water-assisted highly efficient synthesis of impurity-free single-walled carbon nanotubes[J]. *Science*, 2004, 306(5700): 1362-1364.
- [40] Wang S, Zhang L, Xia Z, et al. BCN Graphene as efficient metal-free electrocatalyst for the oxygen reduction reaction [J]. *Angewandte Chemie International Edition*, 2012, 51(17): 4209-4212.
- [41] Jin J, Pan F, Jiang L, et al. Catalyst-free synthesis of crumpled boron and nitrogen co-doped graphite layers with tunable bond structure for oxygen reduction reaction [J]. *ACS Nano*, 2014, 8(4): 3313-3321.
- [42] Zhu J, Jiang S P, Wang R, et al. One-pot synthesis of a nitrogen and phosphorus-dual-doped carbon nanotube array as a highly effective electrocatalyst for the oxygen reduction reaction[J]. *Journal of Materials Chemistry A*, 2014, 2(37): 15448-15453.
- [43] Liang J, Jiao Y, Jaroniec M, et al. Sulfur and nitrogen dual-doped mesoporous graphene electrocatalyst for oxygen reduction with synergistically enhanced performance [J]. *Angewandte Chemie International Edition*, 2012, 51(46): 11496-11500.
- [44] Liu Z, Nie H, Yang Z, et al. Sulfur-nitrogen co-doped three-dimensional carbon foams with hierarchical pore structures as efficient metal-free electrocatalysts for oxygen reduction reactions[J]. *Nanoscale*, 2013, 5(8): 3283-3288.
- [45] Jeon I Y, Choi H J, Choi M, et al. Facile, scalable synthesis of edge-halogenated graphene nanoplatelets as efficient metal-free electrocatalysts for oxygen reduction reaction[J]. *Scientific Reports*, 2013: 3.
- [46] Sun X, Zhang Y, Song P, et al. Fluorine-doped carbon blacks: Highly efficient metal-free electrocatalysts for oxygen reduction reaction[J]. *ACS Catalysis*, 2013, 3(8): 1726-1729.
- [47] Sun X, Song P, Chen T, et al. Fluorine-doped BP 2000: Highly efficient metal-free electrocatalysts for acidic oxygen reduction reaction with superlow  $H_2O_2$  yield [J]. *Chemical Communications*, 2013, 49: 10296-10298.
- [48] Sun X, Song P, Zhang Y, et al. A class of high performance metal-free oxygen reduction electrocatalysts based on cheap carbon blacks[J]. *Scientific Reports*, 2013, 3: 2505.

## Recent Research Progress for Non-Pt-Based Oxygen Reduction Reaction Electrocatalysts in Fuel Cell

SONG Ping<sup>1,2</sup>, RUAN Ming-bo<sup>1,2</sup>, LIU Jing<sup>1,2</sup>, RAN Guang-jun<sup>1,2</sup>, XU Wei-lin<sup>1,2\*</sup>

(1. *State Key Laboratory of Electroanalytical Chemistry, Chinese Academy of Sciences, Changchun 130022, China*; 2. *Jilin Province Key Laboratory of Low Carbon Chemical Power, Changchun Institute of Applied Chemistry, Chinese Academy of Sciences, Changchun 130022, China*)

**Abstract:** The expensive Pt-based catalyst suffers from its susceptibility to time-dependent drift, methanol crossover, and carbon monoxide (CO) deactivation, which will block the large-scale commercial application of fuel cells. It is necessary to develop efficient, low-cost, highly stable non-precious metal oxygen reduction reaction (ORR) catalysts with high catalytic performance. Here, we will pay attention to the research progress of non-precious metal and heteroatom-doped (N, B, P, S, F) metal-free ORR catalysts. Importantly, we mainly focus on the work developed by Xu's group with the Fe-based non-precious metal and F/NF-doped metal-free ORR catalysts. The purpose of these works is to improve the activity and durability of the catalysts based on cheap materials and simple methods. Meanwhile, the combination of theoretical calculations in catalytic activity and mechanism will explain the origin of high activity, which will support strong theoretical foundation for experimental design in ORR catalysts with high performance in future.

**Key words:** oxygen reduction reaction; non-precious metal catalyst; metal-free catalyst; high performance/cost ratio; high stability; catalytic mechanism; theoretical level